

Article

Enhanced Thermoelectric Properties of Polycrystalline SnSe via LaCl₃ Doping

Fu Li ^{1,2}, Wenting Wang ¹, Zhen-Hua Ge ^{1,3,*}, Zhuanghao Zheng ¹, Jingting Luo ¹, Ping Fan ¹ and Bo Li ³

¹ Shenzhen Key Laboratory of Advanced Thin Films and Applications, College of Physics and Energy, Shenzhen University, Shenzhen 518060, China; lifu@szu.edu.cn (F.L.); iimmonkey@qq.com (W.W.); zhengzh@szu.edu.cn (Z.Z.); luojt@szu.edu.cn (J.L.); fanping@szu.edu.cn (P.F.)

² Advanced Materials Institute, Graduate School at Shenzhen, Tsinghua University, Shenzhen 518055, China

³ Faculty of Materials Science and Engineering, Kunming University of Science and Technology, Kunming 650093, China; libo@sz.tsinghua.edu.cn

* Correspondence: ggzh@qq.com; Tel.: +86-0755-2690-5882

Received: 12 January 2018; Accepted: 26 January 2018; Published: 28 January 2018

Abstract: LaCl₃ doped polycrystalline SnSe was synthesized by combining mechanical alloying (MA) process with spark plasma sintering (SPS). It is found that the electrical conductivity is enhanced after doping due to the increased carrier concentration and carrier mobility, resulting in optimization of the power factor at 750 K combining with a large Seebeck coefficient over 300 MvK⁻¹. Meanwhile, all the samples exhibit lower thermal conductivity below 1.0 W/mK in the whole measured temperature. The lattice thermal conductivity for the doped samples was reduced, which effectively suppressed the increment of the total thermal conductivity because of the improved electrical conductivity. As a result, a *ZT* value of 0.55 has been achieved for the composition of SnSe-1.0 wt % LaCl₃ at 750 K, which is nearly four times higher than the undoped one and reveals that rare earth element is an effective dopant for optimization of the thermoelectric properties of SnSe.

Keywords: thermoelectric material; SnSe; electrical conductivity; thermal conductivity

1. Introduction

Thermoelectric (TE) devices can convert waste heat directly and reversibly into electrical energy, which offers a prospect to provide a green and reliable source of energy because they have advantages of no moving parts, no noise, no vibration, and no emission of any harmful gases [1]. The energy conversion efficiency of a TE device is mainly determined by the figure of merit (*ZT*) for a given material, as $ZT = S^2\sigma T/\kappa$, where *S*, σ , κ , and *T* are Seebeck coefficient, electrical conductivity, thermal conductivity, and absolute temperature, respectively. Therefore, to break the bottleneck of the low energy conversion efficiency of TE devices that restricts their widespread application, great effort has been devoted to boosting the performances of the materials by enhancing the *ZT* values via improving the power factor ($S^2\sigma$) and reducing the thermal conductivity in the past decades. Up to now, the *ZT* values have improved over 1.5, and even exceeds 2.0 for the conventional TE materials of PbTe and Bi₂Te₃ based compounds [2–4]. Meanwhile, considering the cost and environmental friendliness of the materials in further application, some competitive compounds [5–7] with non-toxic and inexpensive elements have been sought and found, which has also become an important research point in thermoelectric field in recent years.

Tin selenide (SnSe) with an environmentally friendly composition is recently considered as a very promising TE material because of the high TE property of its single crystal [7–9]. A large *ZT* value over 2.5 was achieved along the *b* direction by combining the anisotropic electrical transport property and the extremely low thermal conductivity caused by the typical layered crystal structure [7]. By further

hole doping, a record high device dimensionless figure of merit ZT_{dev} of 1.34 can be obtained, making it as a robust TE candidate for energy conversion applications [9,10]. However, the layered crystal structure also causes a poor mechanical property of the single crystal, since it can cleave easily along the (001) plane. Moreover, the harsh production conditions are still a disadvantage for practical application. Thereby, more attention has directed to polycrystalline SnSe in recent studies [11–13]. However, it is found that polycrystalline SnSe is much more difficult to yield a high ZT value than its single crystal form due to the higher lattice thermal conductivity and lower electrical transport property originating from the low intrinsic carrier concentration.

For the sake of improving TE performance of polycrystalline SnSe, the study of element substitution at Sn or Se ions is a very important route, because the doping elements always lower the Fermi level to activate multiple valence bands together with introducing point defects and nanoscale precipitates to increase phonon scattering [14]. Thus, the carrier concentration can be optimized while the lattice thermal conductivity can be reduced, resulting in a great enhancement of the ZT value. In fact, the doping effect on SnSe has been extensively investigated in the past work and enhanced TE properties have been achieved by doping with various elements, such as Ag, Na, K, Ag, Pb, Ca, Cu, Br, I, and Ti [12,13,15–20]. For instance, a maximum ZT value of 1.2 was realized for the K and Na codoped SnSe at 773 K. Nevertheless, systematic studies on polycrystalline SnSe doped with rare earth elements with insight into their transport mechanisms are rather scarce so far [21]. In order to develop a useful and comprehensive guide to optimize their TE properties, more studies are needed. Actually, the TE properties of many other compounds have improved by doping rare earth elements due to the optimized carrier concentration and the depressed lattice thermal conductivity [22,23]. In this study, LaCl_3 doped SnSe has been synthesized by combining mechanical alloying (MA) process with spark plasma sintering (SPS), which is as a simple and cost-effective approach used for fabrication of high-performance TE materials in recent years [24–26]. Considering the anisotropic TE transport properties along each crystallographic direction, the electrical and thermal transport properties were investigated along the same direction perpendicular to the SPS pressing direction. It has been found that the electrical properties have been improved and the lattice thermal conductivity can be reduced by doping LaCl_3 , inducing a synergically optimized final TE performance.

2. Materials and Methods

Polycrystalline SnSe- x wt % LaCl_3 ($x = 0.0, 0.5$ and 1.0) samples were synthesized by combining mechanical alloying (MA) and spark plasma sintering (SPS), which is similar to our previous report [18,25]. High-purity starting raw materials Sn (99.999%) and Se (99.999%) with stoichiometric ratio were subjected to MA in argon (>99.5%) atmosphere. After milling for 8 h at 425 rpm in a planetary ball mill, the powders were mixed with LaCl_3 and densified by SPS at 773 K for 5 min in graphite mold with $\Phi 10$ mm. The pressure is 50 MPa with uniaxial during the sintering. Series columnar-shaped specimens with dimensions of $\Phi 10 \times 8$ mm were finally obtained, which were then cut and grinded into special shapes to measure their electrical conductivity, Seebeck coefficient, and thermal conductivity.

The densities of the samples were tested by the Archimedes method. The phase structures were investigated by X-ray diffraction (XRD) with a D/max-RB diffractometer (Rigaku, Tokyo, Japan) using $\text{CuK}\alpha$ radiation via continuous scanning at a scanning rate of $6^\circ/\text{min}$. The microscopic morphology of all the samples were identified with the help of scanning electron microscopy (Zeiss, supra 55 Sapphire, Munich, Germany). The composition of the sample and the distribution of the elements were observed by an energy dispersive X-ray spectrometer (EDS) attached to SEM. Using a Seebeck coefficient/electric resistance measuring system (ZEM-3, Ulvac-Riko, Yokohama, Japan), the Seebeck coefficient and electrical resistance data were recorded concurrently in a temperature range of 300 to 750 K. The Hall coefficients at room temperatures were measured using the van der Pauw technique under a reversible magnetic field of 0.80 T (8400 Series, Model 8404, Lake Shore, Watertown, IL, USA). The thermal diffusivity (D) was measured in the thickness direction of a square-shaped sample of $6 \times 6 \text{ mm}^2$

and 1~2 mm in thickness by using laser flash diffusivity method (LFA467, Netzsch, Selb, Germany). The thermal conductivity (κ) was calculated according to the equation $\kappa = DC_p d$; where C_p is the specific heat capacity obtained from literature. In the literature, the C_p was measured by using a simultaneous thermal analyzer (STA 447, Netzsch, Selb, Germany) [7] and d is the density.

The combined uncertainty of the experimental determination of ZT is about 15~20% and caused by five respective measurements including electrical resistivity, Seebeck coefficient, thermal diffusion coefficient, thermal capacity, and density, at 3~4% for each.

Nomenclature: S , Seebeck coefficient; σ , electrical conductivity; κ , thermal conductivity; κ_c , carrier thermal conductivity; κ_L , lattice thermal conductivity; T , absolute temperature; ZT, the figure of merit; $S^2\sigma$, power factor; SPS, spark plasma sintering; MA, mechanical alloying, XRD, X-ray diffraction; EDS, energy dispersive X-ray spectrometer; SEM, scanning electron microscopy; D , thermal diffusivity; C_p , specific heat; d , density.

3. Results and Discussion

The XRD patterns of all the samples SnSe- x wt % LaCl₃ ($x = 0.0, 0.5$ and 1.0) are shown in Figure 1. As compared with JCPDS data of PDF#48-1224, the patterns of all the compositions can be indexed by SnSe characteristic peaks with layered orthorhombic crystal structure and no second phase is observed within the detection limits of the measurement. However, a slightly stronger intensity of peak (400) with a weaker intensity of peak (100) compared to the standard diffraction peaks can be observed for all the samples, indicating the existence of anisotropy and the preferred orientations occurring along the (400) plane. To confirm the preferred orientation, the preferential factor of all the samples was calculated using the Lotgoering method [25,27], where the bc orientation degree for the ($h00$) crystal planes of the bulk sample is termed as $F_{(h00)}$. When the a -axes of crystal grains are completely aligned along the pressing direction, the calculated value of F is 1. In the present study, the calculated $F_{(h00)}$ values are around 0.34 for all the SnSe- x wt % LaCl₃ ($x = 0.0, 0.5$ and 1.0) samples, which reveals that axial the plane is slightly preferentially oriented in the bc -plane. This is reasonable because SnSe crystallized with layered structure can easily exhibit preferential orientation following the uniaxial densification process, and anisotropy has been widely observed in previous studies [11–13,28].

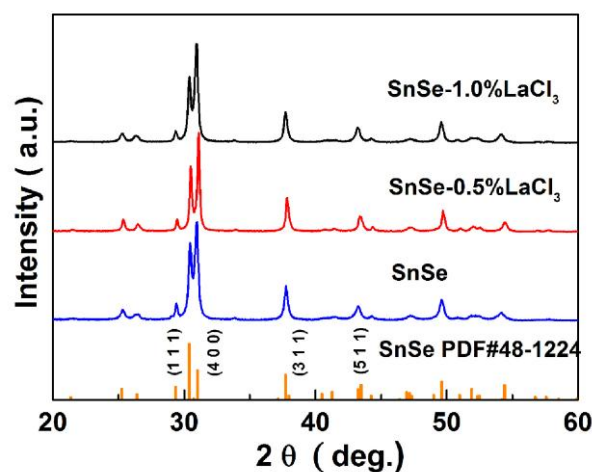


Figure 1. XRD patterns of all the LaCl₃ doped SnSe samples.

SEM morphologies of the fresh fracture surfaces for the samples SnSe-0.5 wt % LaCl₃ and SnSe-1.0 wt % LaCl₃ are presented in Figure 2a,b, respectively. The microstructure of the sample without LaCl₃ was also given in the inset of Figure 2a. It is seen that the undoped sample, with a relative high density over 95% (the theoretical density of SnSe is 6.19 g/cm³), shows a dense morphology. The grain is plate-shaped with size of 1~2 μ m in diameter and 50~100 nm in thickness. However, after

doping, the grain size is reduced to 500 nm~1 μm and decreased as the doping content increased. The plate shaped grains tended to become equiaxed grain due to the reduction of the grain size. It is clear that the reduced grain size is mainly caused by the introduced foreign atoms since they would prevent the diffusion of atoms during the sintering and suppress the growth of grains. Nevertheless, such a fine-grained microstructure is desirable for TE materials, whose thermal conductivity can be reduced by their enhanced phonon scattering due to the increased grain boundaries. In addition, it is also found that the porosity increased when the doped content raised to 1%, which is consistent with the reduced density. This might be caused by some volatilization of Cl. Moreover, the distributions of the elements Sn, Se, La, and Cl on the polished surface of the representative sample SnSe-0.5 wt % LaCl₃ were observed by EDS, which suggests that all the elements are distributed homogeneously.

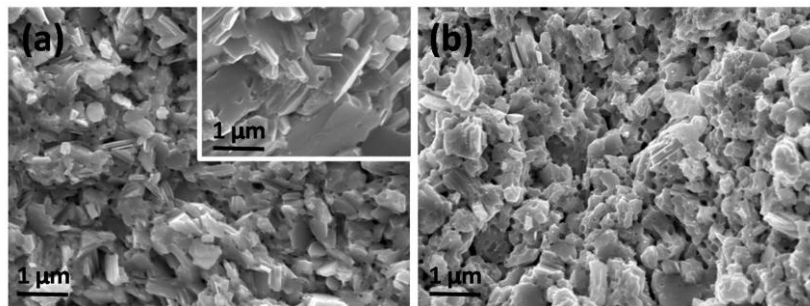


Figure 2. (a) and (b) SEM micrographs of the fresh fracture surfaces for the doped bulks SnSe-0.5 wt % LaCl₃ and SnSe-1.0wt % LaCl₃, respectively. The morphology of the sample without LaCl₃ was given inset of Figure 2a.

Figure 3 shows the electrical transport properties dependence with the measured temperature for all the samples SnSe-*x*wt % LaCl₃ (*x* = 0.0, 0.5 and 1.0), which are measured along the direction perpendicular to the SPS pressing direction since the samples show existence of anisotropy. As shown in Figure 3a, the electrical conductivities of all the samples increase with increasing temperature in the whole measured temperature, indicating a typical semiconducting behavior with nondegenerate characteristics. It is also found that the electrical conductivity for the undoped sample is lower than the doped ones, which shows about $8.53 \times 10^{-4} \text{ Scm}^{-1}$ at room temperature which then increases nearly four orders of magnitude at 750 K, reaching 6.38 Scm^{-1} , which is similar to the previous report [18]. After LaCl₃ doping, the value has improved to about 0.02 Scm^{-1} at room temperature, and then sharply increased in range of 650 to 750 K. An electrical conductivity of 15.55 Scm^{-1} at 750 K is finally obtained, which is two times higher than that of the undoped samples at the same temperature. Additionally, similar electrical conductivities in the whole temperature range were obtained for the samples doped with 0.5% and 1.0% LaCl₃. No obvious differences can be observed with increasing the doped content. The electrical conductivity can be expressed as $\sigma = n\mu e$, where *e* is the unit charge, *n* is the carrier concentration, and μ is the carrier mobility, respectively. Thus, the enhanced electrical conductivity after doping should be ascribed to the increased carrier concentration or the mobility or both of them. The Hall carrier concentration and Hall mobility at room temperature for the samples SnSe and SnSe-0.5 wt % LaCl₃ have been measured. The results indicate that the value of the carrier concentration and carrier mobility for the undoped sample are $7.40 \times 10^{14} \text{ cm}^{-3}$ and $7.23 \text{ cm}^2 \text{ V}^{-1} \text{ s}^{-1}$, respectively. Thus, the lower carrier concentration and carrier mobility should be the reason for the lower electrical conductivity of the undoped sample, which is in agreement with the previous reports [11–13]. However, for the doped sample with 0.5 wt % LaCl₃, the carrier concentration has increased to $1.53 \times 10^{16} \text{ cm}^{-3}$, which is nearly one order of magnitude higher than that of the undoped sample. Meanwhile, the carrier mobility also increases to $12.3 \text{ cm}^2 \text{ V}^{-1} \text{ s}^{-1}$ for the sample with 0.5 wt % LaCl₃. This indicates that the two effects of improvement of both carrier concentration and carrier mobility lead to the enhancement in electrical conductivity, suggesting that LaCl₃ is an effective

dopant in optimizing the electrical transport properties of SnSe. The LaCl_3 doping in SnSe matrix is a strong n -type doping. The La substituting Sn and the Cl substituting Se both increase the electron concentrations in p -type SnSe, but the electrical conductivity of the doped sample is increased. This may be due to the low carrier concentration of the undoped sample. That is, the increasing of electron concentration increased the total carrier concentration as the minority carrier. Furthermore, just a little bit of LaCl_3 should be doped in the SnSe matrix, because of the decreased grain size and increased pores with the increasing LaCl_3 contents observed in SEM images.

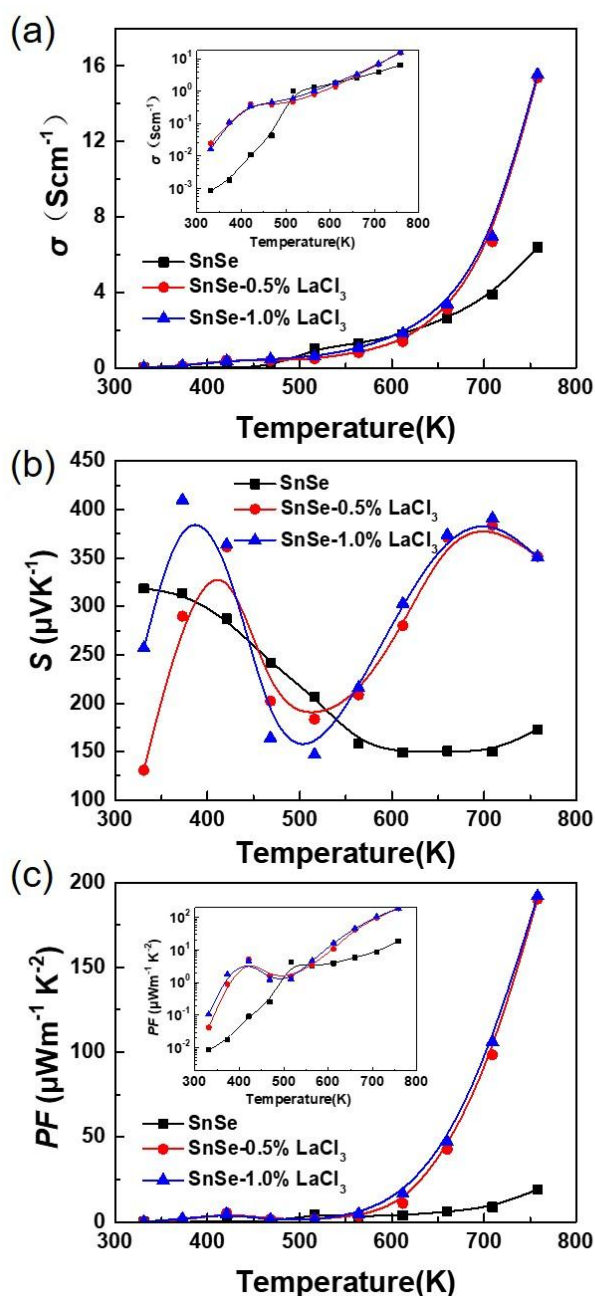


Figure 3. Electrical transport properties as a function of temperature for all the samples $\text{SnSe}-x$ wt % LaCl_3 ($x = 0.0, 0.5,$ and 1.0). (a) electrical conductivity; (b) Seebeck coefficient; (c) power factor.

Figure 3b presents the Seebeck coefficients of all the samples as a function of temperature. The positive values of the Seebeck coefficient for the undoped sample demonstrate a p -type conduction by holes as the dominate carriers. It is also noted that, although it is a n -type doping when LaCl_3 is

doped in SnSe, all the values in the whole temperature range are positive, which is also consistent with the measured Hall coefficient with positive sign. Therefore, this means that a small amount of LaCl₃ substitution cannot change its conductive mechanism. This result is different from the dopant of BiCl₃ in the previous report [29], in which a small amount of dopant can change the conductive mechanism of SnSe from *p*-type to *n*-type. La³⁺ doping and Bi³⁺ doping are all the electron doping (*n* type doping) for SnSe matrix, but the SnSe is an intrinsic *p*-type material due to the Sn vacancies. In this work, the Sn was reduced and we assumed that La³⁺ will stay in the position of Sn for introducing electrons to make the SnSe *n*-type. The results showed that the LaCl₃ could not effectively replace Sn and introduce enough electrons to make the *n*-type change of SnSe compared to BiCl₃, and the reduced Sn will increase Sn vacancies to introduce holes in the matrix and retain the SnSe matrix *p*-type. However, as shown in Figure 3, high absolute Seebeck coefficients over 150 μVK⁻¹ are obtained in the whole measured temperature range for all the samples. For the undoped sample, the Seebeck coefficient decreased as the temperature increased, which is 318 μVK⁻¹ at room temperature, declining to 150 μVK⁻¹ at 750 K, this trend is agreement with the previous report [30]. Nevertheless, the values for all the doped samples have similar strong temperature dependence, which firstly increases and then decreases until 500 K, and further improves as the temperature increases up to 700 K. The Seebeck coefficient is nearly 400 μVK⁻¹ at 700 K and 350 μVK⁻¹ at 750 K, which is two times larger than the undoped sample although the electrical conductivity has enhanced as shown in Figure 3a. The Seebeck coefficient is related to the scattering factor according to the equation $S = \kappa_B / e (\gamma - \ln(n/N_0))$, where *n* and γ are carrier concentration and scattering factor, respectively [25]. The substitution of LaCl₃ can cause structural distortions due to the difference of the ionic radius with SnSe. Thus, the optical phonon may be scattered, causing an improvement of scattering parameter and the Seebeck coefficient. Combing the Seebeck coefficient (*S*) and the electrical conductivity (σ), the power factor ($PF = S^2\sigma$) dependence with temperature was calculated as shown in Figure 3c. All the values increase with increasing temperature in the whole measured temperature range. The power factor below 600 K for all the samples are similar and lower than 25 μWm⁻¹K⁻² because of the poor electrical conductivity. However, benefiting from the enhanced electrical conductivity and Seebeck coefficient over 600 K, the power factor for the doped sample has obviously been enhanced. A maximum value of ~200 μWm⁻¹K⁻² at 750 K is obtained for the LaCl₃ doped sample of SnSe-*x*wt % LaCl₃ with *x* = 0.5 and 1.0, which is nearly an order of magnitude larger than that of the undoped sample.

Figure 4a, b shows the thermal transport properties as a function of temperature for all the samples SnSe-*x* wt % LaCl₃ (*x* = 0.0, 0.5, and 1.0). All the thermal diffusivities are in range of 0.7 to 0.15 mm²/s and decrease gradually as the temperature increases. The changing trend of the thermal conductivity is consistent with that of the thermal diffusivity. For the undoped SnSe, the thermal conductivity at room temperature is 0.94 W/mK. With rising temperature, the value reduces to 0.24 W/mK at 750 K, which is very close to the reported values of the undoped polycrystalline samples [13]. The total thermal conductivity is usually summed by electronic thermal conductivity (κ_e) and lattice thermal conductivity (κ_l), where κ_l is the phonon contribution and κ_e is the electronic contribution which is related to the electrical conductivity according to the Wiedemann–Franz–Lorenz relation, that is $\kappa_e = \sigma LT$, where *L* is Lorenz number, σ is the electrical conductivity, and *T* is the absolute temperature [31]. In the present study, the κ_e holds less than 7% of the total thermal conductivity, revealing that the heat transport of SnSe is predominated by phonon. After doping with 0.5 wt % LaCl₃, the thermal conductivity slightly increases in the whole measured temperature, which decreases with increasing temperature from 0.98 W/mK around room temperature to 0.47 W/mK at 750 K. However, when the doped content increases to 1.0%, the total thermal conductivity reduces, especially in range of 300 to 650 K. Since the electrical conductivity of the undoped sample is lower than the doped ones as shown in Figure 3a, the slightly increased thermal conductivity for the sample with a lower doping content of 0.5% is mainly caused by the improved electronic thermal conductivity. With further increases of the doped content, phonon scattering would be enhanced due to the increased crystal defects introduced by the doping. Thus, the lattice thermal conductivity would further decrease, resulting in a reduction

of the total thermal conductivity for the SnSe-1.0 wt % LaCl_3 sample. Additionally, as discussed above, the grain size is reduced obviously after doping, which would lead to a higher grain boundary concentration for the doped samples. Therefore, phonons would suffer more scattering along grain boundaries, which would induce a lower lattice thermal conductivity and cause a lower total thermal conductivity for the sample doped with 1.0 wt % LaCl_3 than the undoped one.

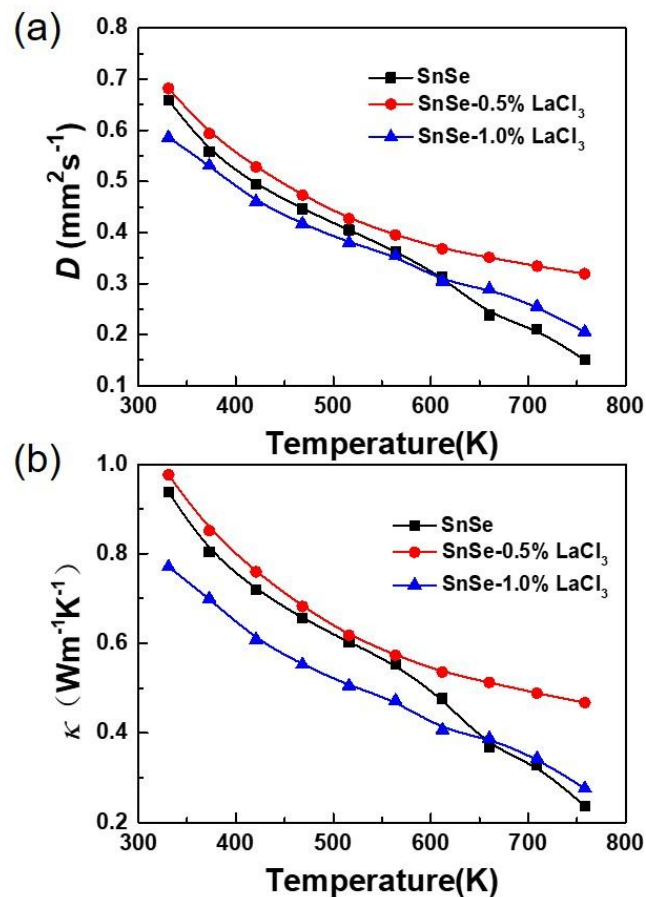


Figure 4. Thermal transport properties as a function of temperature for all the samples SnSe- x wt % LaCl_3 ($x = 0.0, 0.5,$ and 1.0). (a) Thermal diffusivity; (b) thermal conductivity.

The ZT value as shown in Figure 5 was calculated by combining the electrical transport property and thermal conductivity. This shows that the ZT values for all the samples increase with increasing temperature. Because of the lower electrical transport property and higher thermal conductivity, the maximum ZT value for the undoped sample is only 0.15. For all the doped samples, the values are similar to those of the undoped ones in the temperature range of 300 to 600 K. However, attributed to the enhanced electrical conductivity and reduced lattice thermal conductivity with rising the measured temperature after doping, the ZT value is enhanced and a maximum value of 0.55 is obtained for the composition of SnSe-1.0 wt % LaCl_3 at 750 K, which is nearly four times higher than the undoped one. This result suggests that rare earth elements are an effective dopant for improving the TE properties of SnSe.

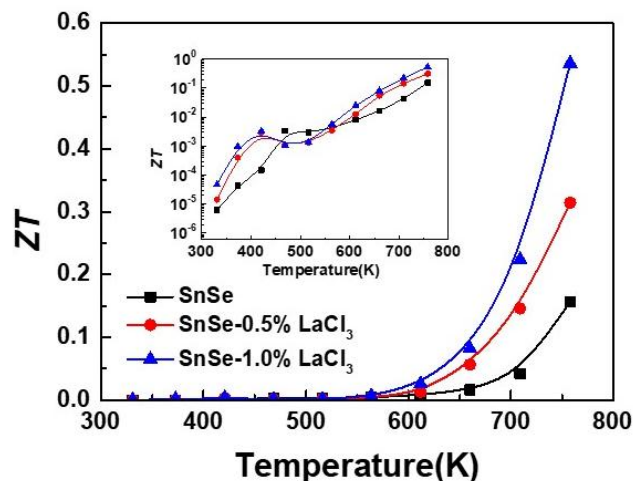


Figure 5. ZT values as a function of temperature for all the samples SnSe- x wt % LaCl₃ ($x = 0.0, 0.5,$ and 1.0).

4. Conclusions

Polycrystalline SnSe- x wt % LaCl₃ ($x = 0.0, 0.5,$ and 1.0) was prepared by combining mechanical alloying (MA) process and spark plasma sintering (SPS). The phase structure and microstructure were observed, and their TE transport properties were investigated in the temperature range of 300 to 750 K. The results indicate that pure phase with a slightly preferred orientation grown along (400) can be obtained for all the samples and the grain size can be reduced after doping. Moreover, the electrical conductivity was improved to 15.55 Scm^{-1} at 750 K for the doped sample because of the increased carrier concentration and carrier mobility, which resulted in an optimization of the power factor combining with the moderate Seebeck coefficient over $300 \mu\text{VK}^{-1}$. Finally, a ZT value of 0.55 has been obtained for the composition of SnSe-1.0 wt % LaCl₃ at 750 K in combination with the reduced thermal conductivity below $1.0 \text{ Wm}^{-1} \text{ K}^{-1}$, which is nearly four times higher than the undoped one.

Acknowledgments: This work was supported by National Nature Science Foundation (grant no. 11764025, 51302140), Shenzhen Science and Technology Plan Project (no. JCYJ20160422102622085, JCYJ20150827165038323), as well as the Natural Science Foundation of SZU (no. 2016016).

Author Contributions: Fu Li prepared the samples; Wenting Wang and Zhuanghao Zheng performed thermoelectric properties measurements; Fu Li and Zhenhua Ge analyzed the data and wrote the paper; Zhenhua Ge, Bo Li, Jingting Luo, and Ping Fan contributed reagents/materials/analysis tools.

Conflicts of Interest: The authors declare no conflict of interest.

References

1. Bell, L.E. Cooling, heating, generating power, and recovering waste heat with thermoelectric systems. *Science* **2008**, *321*, 1457–1461. [[CrossRef](#)] [[PubMed](#)]
2. Pei, Y.Z.; Shi, X.Y.; LaLonde, A.; Wang, H.; Chen, L.D.; Snyder, G.J. Convergence of electronic bands for high performance bulk thermoelectrics. *Nature* **2011**, *473*, 66–69. [[CrossRef](#)] [[PubMed](#)]
3. Wu, H.J.; Zhao, L.D.; Zheng, F.S.; Wu, D.; Pei, Y.L.; Tong, X.; Kanatzidis, M.G.; He, J.Q. Broad temperature plateau for thermoelectric figure of merit $ZT > 2$ in phase-separated PbTe_{0.7}S_{0.3}. *Nat. Commun.* **2014**, *5*, 4515–4524. [[CrossRef](#)] [[PubMed](#)]
4. Kim, S.I.; Lee, K.H.; Mun, H.A.; Kim, H.S.; Hwang, S.W.; Roh, J.W.; Yang, D.J.; Shin, W.H.; Li, X.S.; Lee, Y.H.; et al. Dense dislocation arrays embedded in grain boundaries for high-performance bulk thermoelectrics. *Science* **2015**, *348*, 109–114. [[CrossRef](#)] [[PubMed](#)]
5. Ning, H.; Mastorillo, G.D.; Grasso, S.; Du, B.; Mori, T.; Hu, C.F.; Xu, Y.; Simpson, K.; Maizza, G.; Reece, M.J. Enhanced thermoelectric performance of porous magnesium tin silicide prepared using pressure-less spark plasma sintering. *J. Mater. Chem. A* **2015**, *3*, 17426–17432. [[CrossRef](#)]

6. Khan, A.U.; Kobayashi, K.; Tang, D.M.; Yamauchi, Y.; Hasegawa, K.; Mitome, M.; Xue, Y.M.; Jiang, B.Z.; Tsuchiya, K.; Golberg, D.; et al. Nano-micro-porous skutterudites with 100% enhancement in ZT for high performance thermoelectricity. *Nano Energy* **2017**, *31*, 152–159. [[CrossRef](#)]
7. Zhao, L.D.; Lo, S.H.; Zhang, Y.S.; Sun, H.; Tan, G.J.; Uher, C.; Wolverton, C.; Dravid, V.P.; Kanatzidis, M.G. Ultralow thermal conductivity and high thermoelectric figure of merit in SnSe crystals. *Nature* **2014**, *508*, 373–377. [[CrossRef](#)] [[PubMed](#)]
8. Zhao, L.D.; Chang, C.; Tan, G.J.; Kanatzidis, M.G. SnSe: A remarkable new thermoelectric material. *Energy Environ. Sci.* **2016**, *9*, 3044–3060. [[CrossRef](#)]
9. Zhao, L.D.; Tan, G.J.; Hao, S.Q.; He, J.Q.; Pei, Y.L.; Chi, H.; Wang, H.; Gong, S.K.; Xu, H.B.; Dravid, V.P.; et al. Ultrahigh power factor and thermoelectric performance in hole-doped single-crystal SnSe. *Science* **2016**, *351*, 141–144. [[CrossRef](#)] [[PubMed](#)]
10. Peng, K.L.; Lu, X.; Zhan, H.; Hui, S.; Tang, X.D.; Wang, G.W.; Dai, J.Y.; Uher, C.; Wang, G.Y.; Zhou, X.Y. Broad temperature plateau for high ZTs in heavily doped p-type SnSe single crystals. *Energy Environ. Sci.* **2016**, *9*, 454–460. [[CrossRef](#)]
11. Sassi, S.; Candolfi, C.; Vaney, J.B.; Ohorodniichuk, V.; Masschelein, P.; Dauscher, A.; Lenoir, B. Assessment of the thermoelectric performance of polycrystalline p-type SnSe. *Appl. Phys. Lett.* **2014**, *104*, 212105–212109. [[CrossRef](#)]
12. Chen, C.L.; Wang, H.; Chen, Y.Y.; Day, T.; Snyder, G.J. Thermoelectric properties of p-type polycrystalline SnSe doped with Ag. *J. Mater. Chem. A* **2014**, *2*, 11171–11176. [[CrossRef](#)]
13. Zhang, Q.; Chere, E.K.; Sun, J.Y.; Cao, F.; Dahal, K.; Chen, S.; Chen, G.; Ren, Z.F. Studies on thermoelectric properties of n-type polycrystalline SnSe_{1-x}S_x by iodine doping. *Adv. Energy Mater.* **2015**, *5*, 1500360–1500368. [[CrossRef](#)]
14. Ge, Z.H.; Song, D.S.; Chong, X.Y.; Zheng, F.S.; Jin, L.; Qian, X.; Zheng, L.; Dunin-Borkowski, R.E.; Qin, P.; Feng, J.; et al. Boosting the thermoelectric performance of (Na, K) co-doped polycrystalline SnSe by synergistic tailoring of the band structure and atomic-scale defect phonon scattering. *J. Am. Chem. Soc.* **2017**, *139*, 9714–9720. [[CrossRef](#)] [[PubMed](#)]
15. Wei, T.R.; Tan, G.J.; Zhang, X.M.; Wu, C.F.; Li, J.F.; Dravid, V.P.; Snyder, G.J.; Kanatzidis, M.G. Distinct impact of alkali-ion doping on electrical transport properties of thermoelectric p-type polycrystalline SnSe. *J. Am. Chem. Soc.* **2016**, *138*, 8875–8882. [[CrossRef](#)] [[PubMed](#)]
16. Tang, G.D.; Wei, W.; Zhang, J.; Li, Y.S.; Wang, X.; Xu, G.Z.; Chang, C.; Wang, Z.H.; Du, Y.W.; Zhao, L.D. Realizing high figure of merit in phase-separated polycrystalline Sn_{1-x}Pb_xSe. *J. Am. Chem. Soc.* **2016**, *138*, 13647–13654. [[CrossRef](#)] [[PubMed](#)]
17. Li, D.B.; Tan, X.J.; Xu, J.T.; Liu, G.Q.; Jin, M.; Shao, H.Z.; Huang, H.J.; Zhang, J.F.; Jiang, J. Enhanced thermoelectric performance in n-type polycrystalline SnSe by PbBr₂ doping. *RSC Adv.* **2017**, *7*, 17906–17912. [[CrossRef](#)]
18. Li, F.; Wang, W.T.; Qiu, X.C.; Zheng, Z.H.; Fan, P.; Luo, J.T.; Li, B. Optimization of thermoelectric properties of n-type Ti, Pb co-doped SnSe. *Inorg. Chem. Front.* **2017**, *4*, 1721–1729. [[CrossRef](#)]
19. Gao, J.L.; Xu, G.Y. Thermoelectric performance of polycrystalline Sn_{1-x}Cu_xSe (x = 0–0.03) prepared by high pressure method. *Intermetallics* **2017**, *89*, 40–45. [[CrossRef](#)]
20. Matthews, B.E.; Holder, A.M.; Schelhas, L.T.; Siol, S.; May, J.W.; Forkner, M.R.; Vigil-Fowler, D.; Toney, M.F.; Perkins, J.D.; Gorman, B.P.; et al. Using heterostructural alloying to tune the structure and properties of the thermoelectric Sn_{1-x}Ca_xSe. *J. Mater. Chem. A* **2017**, *5*, 16873–16882. [[CrossRef](#)]
21. Gao, J.L.; Zhu, H.N.; Mao, T.; Zhang, L.B.; Di, J.X.; Xu, G.Y. The effect of Sm doping on the transport and thermoelectric properties of SnSe. *Mater. Res. Bull.* **2017**, *93*, 366–372. [[CrossRef](#)]
22. Liu, Y.C.; Ding, J.X.; Xu, B.; Lan, J.L.; Zheng, Y.H.; Zhan, B.; Zhang, B.; Lin, Y.H.; Nan, C. Enhanced thermoelectric performance of La-doped BiCuSeO by tuning band structure. *Appl. Phys. Lett.* **2015**, *106*, 233903–233908. [[CrossRef](#)]
23. Huang, Y.N.; Zhao, B.C.; Lin, S.; Ang, R.; Song, W.H.; Sun, Y.P. Strengthening of thermoelectric performance via Ir doping in layered Ca₃Co₄O₉ system. *J. Am. Ceram. Soc.* **2014**, *97*, 798–804. [[CrossRef](#)]
24. Wu, J.; Li, F.; Wei, T.R.; Ge, Z.H.; Kang, F.Y.; He, J.Q.; Li, J.F. Mechanical alloying and spark plasma sintering of BiCuSeO oxyselenide: Synthesis process and thermoelectric properties. *J. Am. Ceram. Soc.* **2016**, *99*, 507–514. [[CrossRef](#)]

25. Li, F.; Zheng, Z.H.; Li, Y.W.; Wang, W.T.; Li, J.F.; Li, B.; Zhong, A.H.; Luo, J.T.; Fan, P. Ag-doped SnSe₂ as a promising mid-temperature thermoelectric material. *J. Mater. Sci.* **2017**, *52*, 10506–10516. [[CrossRef](#)]
26. Qin, P.; Qian, X.; Ge, Z.H.; Zheng, L.; Feng, J.F.; Zhao, L.D. Improvements of thermoelectric properties for p-type Cu_{1.8}S bulk materials via optimizing the mechanical alloying process. *Inorg. Chem. Front.* **2017**, *4*, 1192–1199. [[CrossRef](#)]
27. Hao, L.; Feng, N.B.; Jin, Y.R.; Lu, Y. CuAlO₂ thermoelectric compacts by SPS and thermoelectric performance improvement by orientation control. *Ceram. Int.* **2017**, *43*, 12154–12161. [[CrossRef](#)]
28. Chen, W.; Yang, Z.; Lin, F.; Liu, C. Nanostructured SnSe: Hydrothermal synthesis and disorder-induced enhancement of thermoelectric properties at medium temperatures. *J. Mater. Sci.* **2017**, *52*, 9728–9738. [[CrossRef](#)]
29. Wang, X.; Xu, J.T.; Liu, G.Q.; Fu, Y.J.; Liu, Z.; Tan, X.J.; Shao, H.Z.; Jiang, H.C.; Tan, T.Y.; Jiang, J. Optimization of thermoelectric properties in n-type SnSe doped with BiCl₃. *Appl. Phys. Lett.* **2016**, *108*, 083902–083907. [[CrossRef](#)]
30. Chen, Y.; Ge, Z.H.; Yin, M.J.; Feng, D.; Huang, X.Q.; Zhao, W.Y.; He, J.Q. Understanding of the Extremely Low Thermal Conductivity in High-Performance Polycrystalline SnSe through Potassium Doping. *Adv. Funct. Mater.* **2016**, *26*, 6836–6845. [[CrossRef](#)]
31. Khaliq, J.; Jiang, Q.H.; Yang, J.Y.; Simpson, K.; Yan, H.; Reece, M.J. Utilizing the phonon glass electron crystal concept to improve the thermoelectric properties of combined Yb-stuffed and Te-substituted CoSb₃. *Scr. Mater.* **2014**, *72–73*, 63–66. [[CrossRef](#)]



© 2018 by the authors. Licensee MDPI, Basel, Switzerland. This article is an open access article distributed under the terms and conditions of the Creative Commons Attribution (CC BY) license (<http://creativecommons.org/licenses/by/4.0/>).